J. exp. Biol. (1977), **69**, 127–142
With 6 figures
Printed in Great Britain

MECHANICAL ORGANIZATION OF CANTILEVER-LIKE SESSILE ORGANISMS: SEA ANEMONES

BY M. A. R. KOEHL*
Department of Zoology, Duke University, Durham, North Carolina 27706

(*Received* 9 *December* 1976)

SUMMARY

Engineering beam theory has been used to analyse the ways in which body shape and elastic modulus of two species of sea anemones affect their mechanical responses to flow.

1. *Anthopleura xanthogrammica* is exposed to wave action, but because it is short, wide, and thick-walled, maximum tensile stresses in its body walls due to flow forces are an order of magnitude lower than those in the tall, slim, thin-walled, calm-water sea anemone *Metridium senile*.

2. The elastic modulus of *M. senile* body wall is more dependent on extension rate than is that of *A. xanthogrammica*. Because the extension rate of *M. senile* body wall in tidal currents is higher than that of *A. xanthogrammica* in wave surge, the moduli of walls from these species when exposed to such flow conditions are similar, between 0·1 and 0·3 $MN.m^{-2}$.

3. The flexural stiffness of *M. senile* is lowest in the upper column where the anemones bend in currents: this orients their filter-feeding oral discs normal to the currents. The flexural stiffness of *A. xanthogrammica* is one to two orders of magnitude higher than that of *M. senile*; *A. xanthogrammica* remain upright in wave surge and feed on mussels that fall on their oral discs.

4. The deflexions of these anemones predicted using beam theory are consistent with those observed in nature.

5. The critical stress to produce local buckling is an order of magnitude lower for *M. senile* than for *A. xanthogrammica*.

6. Several general principles of the organization of cantilever-like sessile organisms are revealed by this study of sea anemones.

INTRODUCTION

The shape of a structure determines the distribution of mechanical stress (force per cross-sectional area) within the structure for a given load distribution. The rigidity of the materials comprising a structure determines how much it will deform in response to stresses. Thus, the ability of an organism to resist deformation by an imposed load depends upon both the shape of its body and the mechanical properties of its tissues. This paper describes how aspects of body shape and material can maximize or minimize the deformation of an organism when it is loaded.

Sea anemones are basically hydrostatically supported cylinders attached at one end to the substratum. Large *Metridium senile fimbriatum* (Verrill) are subtidal anemones

* Present address: Friday Harbor Laboratories, Friday Harbor, Washington 98250.

that are bent over by slow tidal currents and filter-feed through their lobed oral discs (Koehl, 1976). In contrast, *Anthopleura xanthogrammica* (Brandt) are intertidal anemones that remain upright when exposed to wave action (Koehl, 1976) and feed on mussels that fall on their oral discs (Dayton, 1973). Since the same flow force that causes *M. senile* to bend over does not noticeably deform an *A. xanthogrammica* (Koehl, 1976), I expected that the latter would have a more stress-minimizing shape and/or a stiffer body wall than the former.

A sessile anemone can be considered as a cantilevered beam supporting a feeding apparatus in flowing water in a suitable orientation for food capture. A cantilevered beam (sea anemone) subjected to a load (flow force) undergoes shearing (Fig. 1A) and bending (Fig. 1B). The oral disc of an anemone deformed in shearing remains parallel to the substratum and the flow direction, whereas the oral disc of an anemone deformed in bending does not.

I used beam theory (which is discussed in Faupel, 1964; Alexander, 1968; and Wainwright *et al.* 1976) to analyse the effects of body shape and materials on the mechanical responses of *M. senile* and *A. xanthogrammica* to flow forces.

MATERIALS AND METHODS

M. senile along the Pacific coast of North America range from small, shallow-water anemones with large tentacles to large, deeper-water animals with lobed oral discs covered with numerous small tentacles (Hand, 1955*b*). The present study is concerned only with the latter form of *M. senile*. Although a few individuals of *A. xanthogrammica* can be found in the more protected coastal sites, they are most abundant in exposed surge channels (Koehl, 1976), and it is these animals that were used in the present study.

The heights above the substratum and the diameters at various points along the bodies of expanded *A. xanthogrammica* were measured to the nearest 5 mm in the field. To minimize sampling bias, I measured every anemone encountered in a tide pool or surge channel. The heights and diameters of expanded *M. senile* were measured to the nearest 5 mm on photographs of the anemones with a centimetre grid held next to them. To minimize sampling bias, the groups of anemones to be photographed were chosen in a haphazard manner and all expanded individuals whose entire bodies were visible in a photograph were measured. Nine *M. senile* and 17 *A. xanthogrammica* were anaesthetized in solutions of 20% $MgSO_4.7H_2O$ one to one with Instant Ocean (Pantin, 1964) and strips were cut from the columns of relaxed anemones with a razor blade. The thickness of such strips was measured to the nearest 0·1 mm.

Anemones of both species were collected and kept in refrigerated aquaria containing Instant Ocean. Every fourth day, *M. senile* were fed brine shrimp nauplii and *A. xanthogrammica* were fed mussels or snails. Only the body walls of actively posturing animals that responded to food were used for mechanical testing. Chapman (1953) observed that the passive mechanical behaviour of anemone body wall depends on the connective tissue but not the muscles of the body wall. I therefore used relaxed strips of body wall for mechanical tests and did not risk damaging the delicate strips by attempting to remove the muscle fibres. The strips were pulled at various rates in

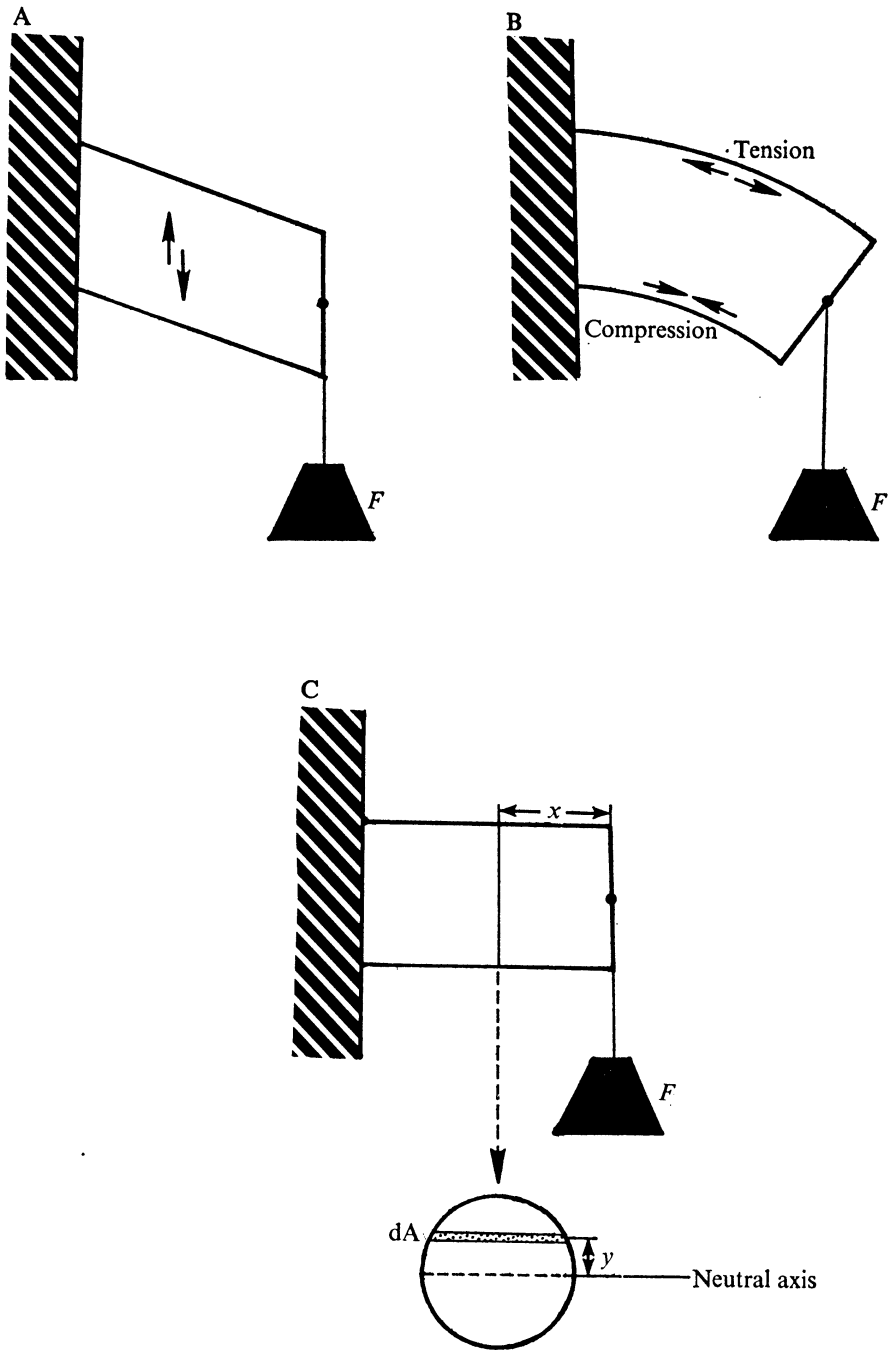

Fig. 1. Diagram of a cantilevered beam supporting a load (F). (A) Deformation in shearing, (B) deformation in bending (the arrows in (A) and (B) indicate the directions in which molecules of the beam are tending to be moved), (C) side view of the beam and cross-section of the beam at distance x from the free end of the beam. The unit of area dA is at distance y from the axis of bending of the beam.

an Instron Universal Testing Instrument (Model TT-C) that simultaneously recorded force (standard error, S.E. = ±0·5%) and extension (S.E. = ±0·25%). The strips were attached with contact cement (Eastman 9–10) to two stainless-steel spring clamps which were gripped in the Instron. The length between the grips, the width, and the thickness of each strip was measured to the nearest 0·1 mm using callipers. The strips being pulled were immersed in a bath of the anaesthetic solution kept at 10 °C by an ice jacket (water temperatures in areas along the coast of Washington where the anemones are found range from 5 to 16 °C (Connell, 1970)). Plots of stress versus extension (the ratio of change in length of the specimen to its original unstressed length) were made. The slope of the straight portion of each such stress-extension curve was taken to be the modulus of elasticity (E) for that specimen.

RESULTS AND DISCUSSION

Body shape

M. senile are tall (mean height above the substratum = 38·0 cm, standard deviation, S.D. = 9·0, number of measurements, n = 28) and slim (expanded *M. senile* are roughly three times taller than they are wide) (Table 1). *M. senile* columns taper, being narrowest about three-quarters of the column height above the substratum. In contrast *A. xanthogrammica* are short (mean height = 2·5 cm, S.D. = 0·9, n = 71) and squat (expanded *A. xanthogrammica* in surge channels are roughly three times wider than they are tall) (Table 2).

A. xanthogrammica body walls are twice as thick as those of *M. senile*; the mean body-wall thickness measured at mid-column height of *A. xanthogrammica* is 2·2 mm and of *M. senile* is 1·1 mm. This difference in thickness is significanct ($F_{[1,\ 200]}$ = 228·7, $P < 0{\cdot}001$). The body walls of both species are thicker towards the base (Fig. 2) where the bending moments caused by flow forces are greatest.

The second moments of area (I, a measure of the distribution of material around the axis of bending) of typical *M. senile* and *A. xanthogrammica* are calculated in the Appendix and listed in Table 3. The I of the lower column of *M. senile* is of the same order of magnitude as that of *A. xanthogrammica*; although the body wall of *A. xanthogrammica* is thicker, the diameter of the *M. senile* lower column is greater. The I of the thin-walled, narrow upper column of a typical *M. senile* is an order of magnitude lower, however, than that of the lower column.

Shear stresses and tensile stresses

The shear stresses and the tensile stresses associated with bending are calculated in the Appendix and listed in Table 3 for typical *M. senile* in tidal current and *A. xanthogrammica* in wave surge. Shear stresses are minimized in beams with large cross-sectional areas, but are independent of cross-sectional shape. In contrast, tensile stresses associated with bending are minimized when the most material is the greatest possible distance from the axis of bending (i.e. when I is high). The shear stresses in *M. senile* are of the order of $10^3\ \mathrm{N.m^{-2}}$ whereas the maximum tensile stresses are of the order of $10^4\ \mathrm{N.m^{-2}}$. If a cantilever has a uniform cross-sectional shape, maximum stresses occur near the base of the beam; in *M. senile*, however,

Table 1. *Body proportions of expanded* Metridium senile

H = height of anemone
h = height of oral disc
L = height of column
OD = diameter of oral disc (tentacle tip to tentacle tip)
C_1 = diameter of column just below capitulum
C_2 = diameter of column 3/4 of column height above substratum
C_3 = diameter of column 1/2 of column height above substratum
C_4 = diameter of column 1/4 of column height above substratum
PD = diameter of pedal disc

(See Fig. 6*a*)

Proportion	Mean ($\bar{x}$)	(S.D.)	Sample size (n)
PD/H	0·31	0·11	33
OD/PD	1·78	0·35	35
C_1/PD	0·56	0·07	27
C_2/PD	0·46	0·08	27
C_3/PD	0·54	0·08	27
C_4/PD	0·71	0·09	27
h/L	0·39	0·06	17

Table 2. *Body proportions of expanded* Anthopleura xanthogrammica

H = height of anemone
h = height of oral disc and widened region of upper column
OD = diameter of oral disc (tentacle tip to tentacle tip)
PD = diameter of pedal disc
t = length of tentacle

(See Fig. 6*c*)

Proportion	Mean ($\bar{x}$)	(S.D.)	Sample size (n)
OD/H*	3·80	1·17	70
OD/PD	1·54	0·27	12
t/OD	0·16	0·03	9
h/PD	0·17	0·04	14

**Anthopleura xanthogrammica* in protected sites have a mean OD/H of 1·81 (S.D. = 0·41, n = 19).

maximum stresses occur at the narrow region of the upper column where I is lowest. The shear and maximum tensile stresses in *A. xanthogrammica* are only between $10^2\,N.m^{-2}$ and $10^3\,N.m^{-2}$, with shear stresses being greater. Thus, although *A. xanthogrammica* is exposed to wave action, because it is short and wide, the maximum tensile stresses in its body wall due to flow forces are an order of magnitude lower than those in a tall, calm-water *M. senile*. Note that although the I of the lower column of the typical *M. senile* is slightly greater than that of the *A. xanthogrammica*, the tensile stresses in the former are nearly 20 times larger than in the latter, because *M. senile* is taller.

M. senile and *A. xanthogrammica* illustrate the profound effect that body height and cross-sectional dimensions can have on the magnitude and distribution of stresses in beam-like organisms subjected to loads such as flow forces.

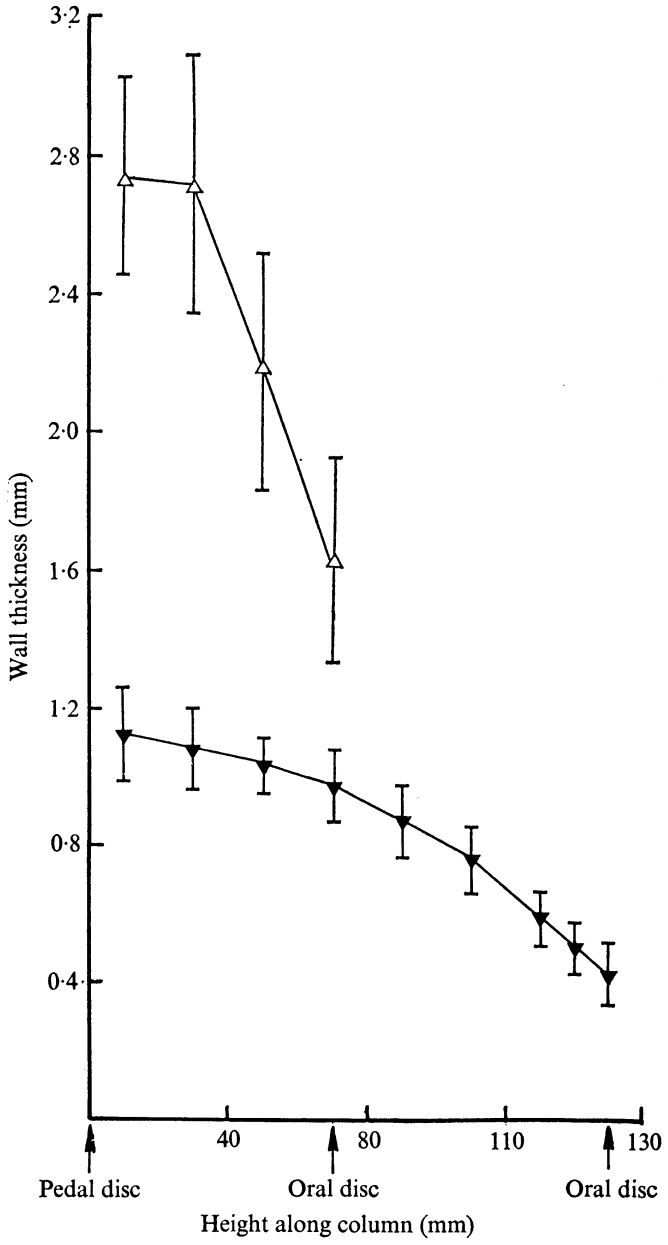

Fig. 2. Graph of the thickness of body wall at various heights along the columns of an *A. xanthogrammica* (△) and a *M. senile* (▼). Twelve strips the length of the column were cut from each anemone and the thickness at 1-cm intervals along the strips were measured. Error bars indicate standard deviation.

Material rigidity

Representative graphs of the stress in strips of body wall from *M. senile* and *A. xanthogrammica* at various extensions are shown in Fig. 3. Note that the stress-extension curves for both species have steeper slopes when extension rate (change in length per original length per s) is higher. This indicates that the faster the anemone body wall is stretched, the higher is its modulus of elasticity (*E*). This increase in

Table 3. *Calculated stresses in and deflexions of sea anemones in flowing water*

	M. senile	*A. xanthogrammica*
Type of flow	Tidal current (0·2 $m.s^{-1}$ at the oral disc)	Wave surge (0·2 $m.s^{-1}$ at the oral disc)
Second moment of area (I)	$3{\cdot}0 \times 10^{-8}$ m^4 (upper column) $6{\cdot}9 \times 10^{-7}$ m^4 (lower column)	$2{\cdot}0 \times 10^{-7}$ m^4
Shear stress (σ_S)	$4{\cdot}4 \times 10^{3}$ $N.m^{-2}$ (upper column) $1{\cdot}5 \times 10^{3}$ $N.m^{-2}$ (lower column)	$9{\cdot}1 \times 10^{2}$ $N.m^{-2}$
Maximum bending tensile stress (σ_T)	$3{\cdot}9 \times 10^{4}$ $N.m^{-2}$ (upper column) $1{\cdot}3 \times 10^{4}$ $N.m^{-2}$ (lower column)	$9{\cdot}5 \times 10^{2}$ $N.m^{-2}$
Flexural stiffness (EI)	$5{\cdot}1 \times 10^{-3}$ $N.m^2$ (upper column) $1{\cdot}2 \times 10^{-1}$ $N.m^2$ (lower column)	$5{\cdot}1 \times 10^{-2}$ $N.m^2$
Linear deflexion of oral disc (δ)	8×10^{-2} m	$1{\cdot}3 \times 10^{-5}$ m
Critical stress for local buckling (σ_L)	$7{\cdot}9 \times 10^{2}$ $N.m^{-2}$	$4{\cdot}5 \times 10^{3}$ $N.m^{-2}$

rigidity with increased extension rate is more pronounced for *M. senile* body wall than for *A. xanthogrammica* body wall.

Analyses of variance reveal that for an individual anemone at each of the extension rates used there is no significant difference between the elastic moduli of strips of body wall from the same or from different regions of the column (upper, middle, or lower column), or between moduli of strips of body wall pulled along different axes (longitudinal or circumferential axes of the anemone). Moduli of strips of body wall from different individuals of the same species pulled at a given strain rate are in some instances significantly different ($0{\cdot}025 < P < 0{\cdot}05$), but the coefficients of determination are low (0·01 or less). All elastic modulus data is pooled for each species to graph modulus against extension rate. Such graphs indicate that modulus has a power law relationship to extension rate, hence a log-log plot of elastic modulus against extension rate for each species should yield a straight line (Fig. 4). Analysis of covariance reveals that the regression line fitted to the data for *A. xanthogrammica* and that for *M. senile* are significantly different in slope ($F_{[1,182]} = 6{\cdot}80$, $0{\cdot}01 < P < 0{\cdot}025$) and in elevation ($F_{[1,183]} = 7{\cdot}40$, $0{\cdot}005 < P < 0{\cdot}01$). By converting the equations from their logarithmic form (Fig. 4) to their power law form, the relationship between modulus and extension rate for *M. senile* body wall becomes

$$E = 1{\cdot}11(\dot{\epsilon})^{0.29}, \tag{1}$$

and for *A. xanthogrammica* body wall,

$$E = 0{\cdot}94(\dot{\epsilon})^{0.16}, \tag{2}$$

where E is elastic modulus in $MN.m^{-2}$ and $\dot{\epsilon}$ is extension rate in s^{-1}. Note that because the modulus of *M. senile* wall is more dependent on extension rate than that of *A. xanthogrammica* wall, at high extension rates (between 0·1 s^{-1} and 1·0 s^{-1}) *M. senile* is as rigid as *A. xanthogrammica*, but at slower extension rates (lower than 0·001 s^{-1}) *A. xanthogrammica* is significantly more rigid than *M. senile* ($F_{[1,29]} = 25{\cdot}62$, $P < 0{\cdot}001$).

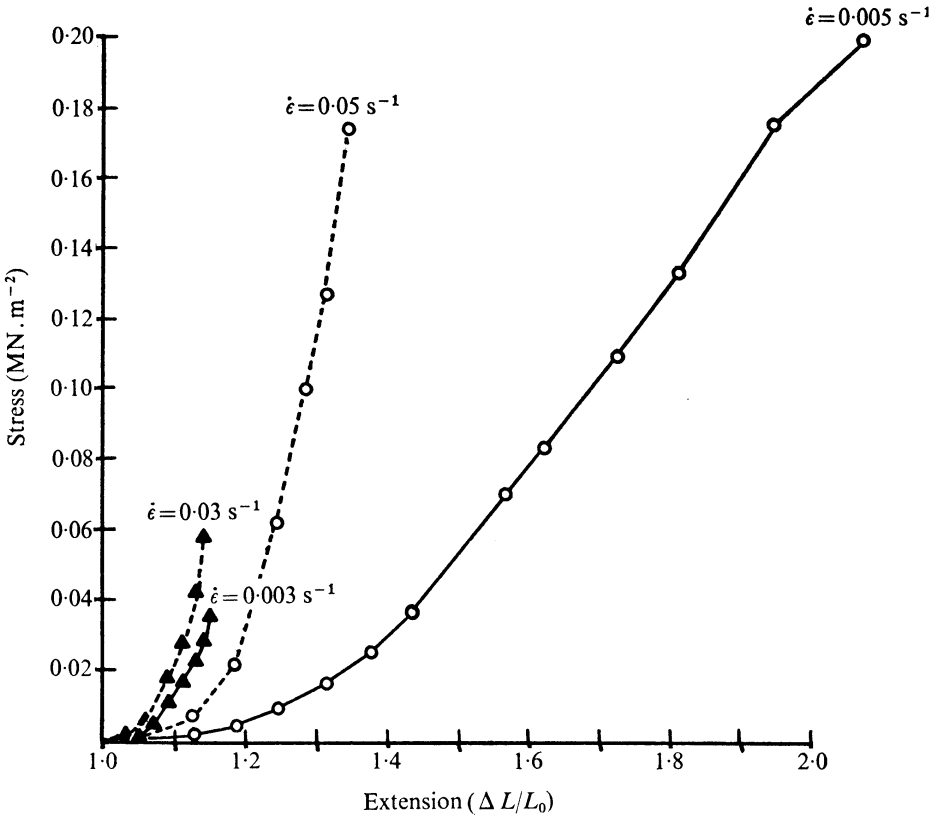

Fig. 3. Graphs of stress ($MN.m^{-2}$) against extension (the ratio of the increase in length to the original length of the specimen) for strips of body wall from a *M. senile* (○) and an *A. xanthogrammica* (▲) pulled along their longitudinal axes in an Instron testing machine at a rapid (dashed line) and a slow (solid line) extension rate ($\dot{\epsilon}$).

The deformations of these two species of anemones depend upon the elastic moduli of their body walls, which in turn depend upon the rates at which they are stretched. Therefore, the extension rates of the animals' body walls when subjected to flow forces must be assessed before their mechanical responses to those forces can be predicted. These extension rates can be estimated by doing 'creep' tests (Koehl, 1977*b*). In a creep test, a relaxed strip of *M. senile* body wall can be subjected to longitudinal stress of the order of $10^4\ N.m^{-2}$ to simulate the maximum tensile stresses it experiences in tidal currents. The slope of the straight portion of a plot of extension of the strip against time should be a reasonable estimate of the extension rate of the anemone wall. The mean extension rate of *M. senile* body wall subjected to stresses between $3{\cdot}0\times10^4\ N.m^{-2}$ and $7{\cdot}5\times10^4\ N.m^{-2}$ is $0{\cdot}0016\ s^{-1}$ (S.D. = 0·0004, n = 11). Therefore, by equation (1) an estimate of the elastic modulus of the body wall of a *M. senile* in a tidal current is $0{\cdot}17\ MN.m^{-2}$. When *A. xanthogrammica* body wall is subjected to longitudinal stresses between $0{\cdot}6\times10^3\ N.m^{-2}$ and $1{\cdot}7\times10^3\ N.m^{-2}$ to simulate stresses due to wave surge, the mean extension rate is only $0{\cdot}00025\ s^{-1}$ (S.D. = 0·00024, n = 21) and the calculated modulus (by equation 2) is $0{\cdot}25\ MN.m^{-2}$. *A. xanthogrammica* walls in surge extend at a rate roughly ten times lower than do *M. senile* walls in tidal currents; hence, because the elastic modulus of anemone body

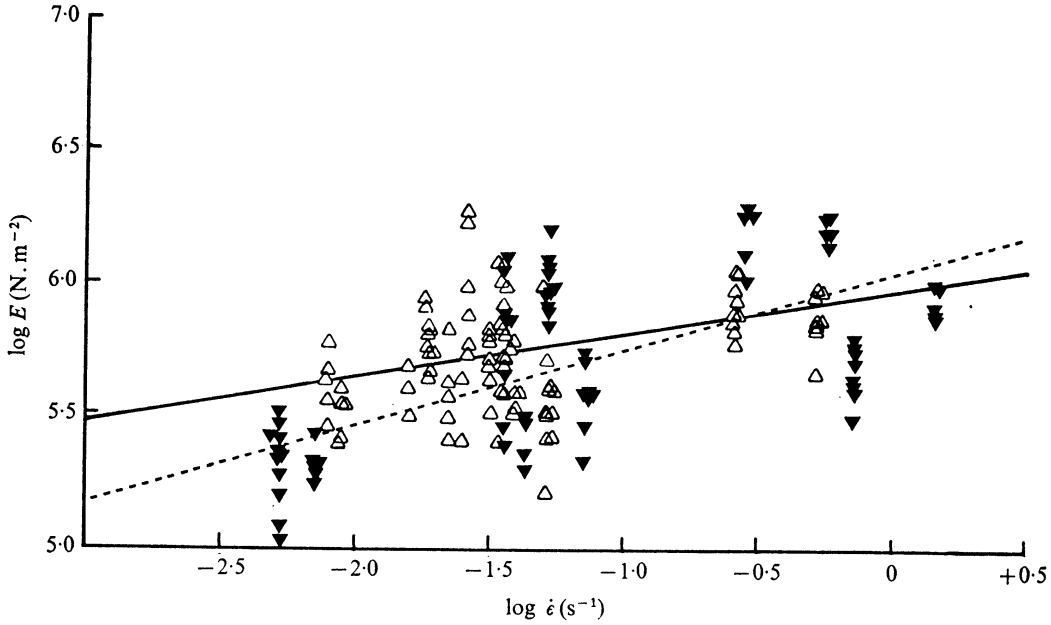

Fig. 4. Graph of the log of elastic modulus (N.m^{-2}) against the log of extension rate (s^{-1}) for *M. senile* body wall (▼) and *A. xanthogrammica* body wall (△). The dashed line represents the regression line fitted by the least squares method to the set of data points for *M. senile*, and the solid line represents the regression line fitted to the data points for *A. xanthogrammica*.

wall depends upon extension rate, the walls of *M. senile* in tidal currents are as rigid as those of *A. xanthogrammica* in surge, even though *A. xanthogrammica* walls are stiffer at a given extension rate (when $\dot{\epsilon} < 0{\cdot}01$ s^{-1}).

Flexural stiffness

An index for the resistance of a beam to being bent by a load is flexural stiffness, the product of E (a material property) and I (a shape property). The EI of a typical *M. senile* and a typical *A. xanthogrammica* are calculated in the Appendix and listed in Table 3. Note that the flexural stiffness of the upper column of *M. senile* is roughly 20 times lower than that of the lower column. Since body wall from any location in the *M. senile* column has the same modulus, the local increase in flexibility at the upper column is due to shape. It is not surprising that *M. senile* in a current is bent at this upper region of its column; the anemone's filter-feeding oral disc is thus oriented normal to the direction of flow and is held out in the more rapidly flowing water away from the substream.

The flexural stiffness of a typical *A. xanthogrammica* in surge is an order of magnitude greater than that of the upper column of a *M. senile* in a tidal current, again due to a difference in cross-sectional shape. In particular cases where the extension rate on the wall of *A. xanthogrammica* is greater than that mentioned above, the elastic modulus of the *A. xanthogrammica* body wall is higher than that of *M. senile* wall; in such cases the difference between the flexural stiffnesses of the two species becomes greater and is due to differences in both shape and material rigidity (Koehl, 1976). *A. xanthogrammica*

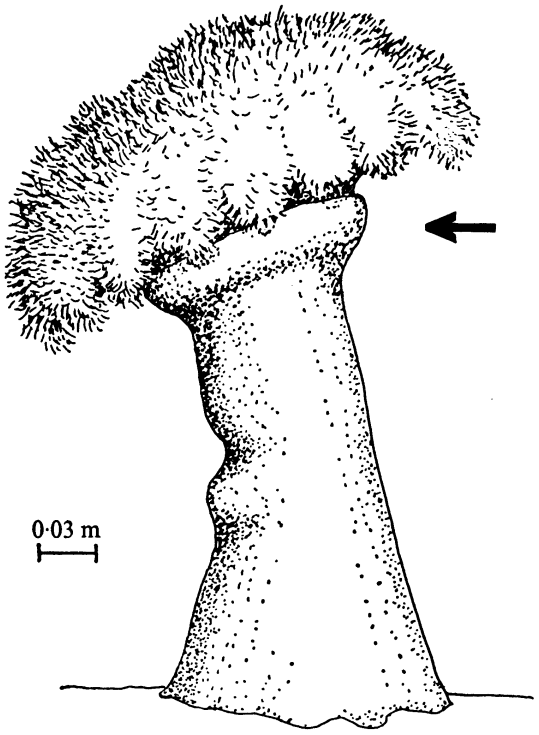

Fig. 5. Tracing of a photograph of a *M. senile* that has undergone local buckling. The arrow indicates the direction of the tidal current.

do not bend visibly in moving water; their oral discs remain upright where mussels are more likely to fall on them.

Deflexion

The linear deflexion of the free end (oral disc) of a typical *M. senile* deformed by a tidal current and of a typical *A. xanthogrammica* deformed by surge can be predicted using beam theory (Appendix). The predicted deflexions (Table 3) are consistent with deflexions of the anemones observed in the field.

Local buckling

A beam may undergo local buckling, i.e. may kink as a drinking straw does when bent too far. Such buckling reduces the size of the lumen of a hollow beam and thus is resisted if the beam is filled with fluid under pressure. However, because the internal pressures of sea anemones are only of the order of 0·1–10 cm H_2O (Chapman, 1974), I have considered anemones to be open tubes as a first approximation to calculate the critical stress to produce local buckling (Appendix).

The lower columns of *M. senile* in tides and *A. xanthogrammica* in surge have roughly the same flexural stiffness. However, because *A. xanthogrammica* columns are thicker-walled and *M. senile* lower columns are larger in diameter, the critical stress to produce local buckling is an order of magnitude greater for *A. xanthogrammica* than for *M. senile* (Table 3). This critical stress falls within the range of stresses

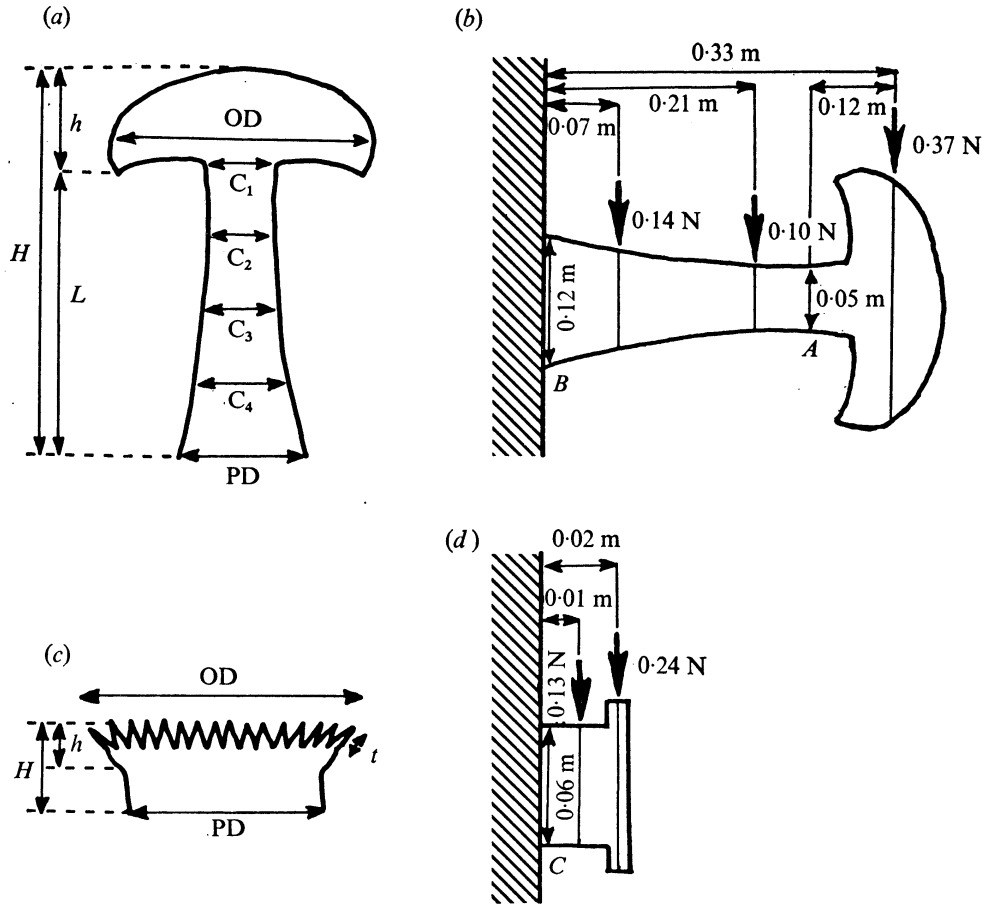

Fig. 6. Diagrams of (*a*) *M. senile* (symbols used in Table 1), (*b*) 'typical' *M. senile* exposed to flow forces (see Appendix), (*c*) *A. xanthogrammica* (symbols used in Table 2), (*d*) 'typical' *A. xanthogrammica* exposed to flow forces (see Appendix).

M. senile encounter in the field, and in fact buckled *M. senile* are observed in the field (Fig. 5).

Mechanical organization of cantilever-like sessile organisms

By analysing the ways in which body shape and elastic modulus of two species of sea anemones affect their mechanical responses to flow, several general principles of the organization of cantiliver-like sessile organisms are revealed:

(1) Tall, slim shapes tend to maximize the stresses in a body for a given load distribution, whereas short, wide shapes tend to minimize the stresses for a given load distribution.

(2) The rigidity (elastic modulus) of the materials from which an organism is built can depend upon how fast the materials are stretched, which depends upon the magnitude of the stresses to which they are subjected, which in turn depend upon the shape of the organism.

(3) Flexural stiffness is the ability of a beam-like organism to resist bending. The higher the elastic modulus of the organism's tissues and the greater the distance of

those tissues from the axis of bending, the less the organism will bend when loaded.

(4) A beam-like organism can be flexible at a specific region of its body by reducing the diameter (and/or wall thickness if it is hollow) of that region of the body, and/or by reducing the elastic modulus of the tissue there. Thus, a narrow region in a beam-like body can behave like a flexible joint (Wainwright & Koehl, 1976).

(5) If a hollow beam-like organism becomes too wide or thin-walled, it is liable to kink when loaded.

This work, which was supported by a Cocos Foundation Training Grant in Morphology, a Theodore Roosevelt Memorial Fund of the American Museum of Natural History Grant, and a Graduate Women in Science Grant, was the direct result of a most stimulating association with S. A. Wainwright. I gratefully acknowledge his advice and enthusiasm. I thank G. Pearsall for his advice and the Department of Mechanical Engineering, Duke University, for the use of their Instron. I am grateful to T. Suchanek for supplying me at Duke with freshly collected anemones from the Pacific, and to D. Crenshaw for his advice on statistical analyses.

REFERENCES

ALEXANDER, R. McN. (1968). *Animal Mechanics*. Seattle: University of Washington Press.

CHAPMAN, G. (1953). Studies of the mesoglea of coelenterates. II. Physical properties. *J. exp. Biol.* **30**, 440–51.

CHAPMAN, G. (1974). The skeletal system. In *Coelenterate Biology: Reviews and New Perspectives* (ed. L. Muscatine), pp. 93–128. New York: Academic Press.

CONNELL, J. H. (1970). A predator–prey system in the marine intertidal region. I. *Balanus glandula* and several predatory species of *Thais*. *Ecol. Monogr.* **40**, 49–78.

DAYTON, P. K. (1973). Two cases of resource partitioning in an inter-tidal community: making the right prediction for the wrong reason. *Am. Nat.* **107**, 662–70.

FAUPEL, J. H. (1964). *Engineering Design*. New York: John Wiley and Sons, Inc.

HAND, C. (1955*a*). The sea anemones of central California. II. The Corallimorpharian and Athenarian anemones. *Wasmann J. Biol.* **12**, 345–75.

HAND, C. (1955*b*). The sea anemones of central California. Part III. The Acontiarian anemones. *Wasmann J. Biol.* **13**, 189–251.

KOEHL, M. A. R. (1967). Mechanical design in sea anemones. In *Coelenterate Ecology and Behaviour* (ed. G. O. Mackie), pp. 23–31. New York: Plenum Publishing Corp.

KOEHL, M. A. R. (1977*a*). Effects of sea anemones on the flow forces they encounter (submitted to *J. exp Biol.*)

KOEHL, M. A. R. (1977*b*). Mechanical diversity of connective tissue of the body wall of sea anemones. (submitted to *J. exp. Biol.*)

PANTIN, C. F. A. (1964). *Notes on Microscopical Technique for Zoologists*. Cambridge University Press.

WAINWRIGHT, S. A., BIGGS, W. D., CURREY, J. D. & GOSLINE, J. M. (1976). *Mechanical Design in Organisms*. New York: John Wiley and Sons.

WAINWRIGHT, S. A. & KOEHL, M. A. R. (1976). The nature of flow and the reaction of benthic cnidaria to it. In *Coelenterate Ecology and Behaviour* (ed. G. O. Mackie), pp. 5–21. New York: Plenum Publishing Corp.

APPENDIX. SAMPLE CALCULATIONS OF STRESSES IN AND DEFLEXIONS OF SEA ANEMONES

The body dimensions of a 'typical' *M. senile* (Fig. 6*b*) were calculated from the mean height of *M. senile* measured in the field ($\bar{x}$ = 0·38 m, S.D. = 0·09, n = 28) using the body proportions listed in Table 1. The flow forces (heavy arrows) on the oral disc, upper column, and lower column were calculated using field measurements of flow velocities over *M. senile* (Koehl, 1977*a*) and are assumed to act on the midpoint of each of the three portions of the body.

The body dimensions of a 'typical' *A. xanthogrammica* (Fig. 6*d*) were calculated from the mean height of *A. xanthogrammica* in exposed surge channels ($\bar{x}$ = 0·025 m, S.D. = 0·009, n = 71) using the proportions listed in Table 2. The flow forces (heavy arrows) on the oral disc and the column were calculated using field measurements of flow velocities over *A. xanthogrammica* in exposed surge channels (Koehl, 1977*a*) and are assumed to act on the midpoint of each of these two portions of the body.

1. *Second moment of area* (I)

The anemone is considered to be a hollow cylindrical cantilever, and thus I is given by

$$I = \frac{\pi (r_1^4 - r_2^4)}{4}, \tag{3}$$

where r_1 is the outer radius of the cylinder and r_2 is the inner radius ($r_2 = r_1 - t$, where t is the thickness of the cylinder wall). In *M. senile* and *A. xanthogrammica* the contribution to I of the mesenteries is small because they are very thin relative to the body wall (see Hand, 1955*a*, *b*) and are closer to the axis of bending. Therefore, the mesenteries are neglected for simplicity's sake in the following calculations.

M. senile. The mean wall thickness of *M. senile* body wall from the narrow region of the upper column (indicated by A in Fig. 6*b*) is 5×10^{-4} m (S.D. = 1×10^{-4}, n = 45), and from the lower column (B in Fig. 6*b*) is $1{\cdot}1 \times 10^{-3}$ m (S.D. = $0{\cdot}2 \times 10^{-3}$, n = 45), hence

$$I_A = \frac{\pi[(2{\cdot}70 \times 10^{-2}\ \text{m})^4 - (2{\cdot}65 \times 10^{-2}\ \text{m})^4]}{4},$$
$$= 3 \times 10^{-8}\ \text{m}^4,$$

and

$$I_B = \frac{\pi[(5{\cdot}90 \times 10^{-2}\ \text{m})^4 - (5{\cdot}79 \times 10^{-2}\ \text{m})^4]}{4},$$
$$= 6{\cdot}9 \times 10^{-7}\ \text{m}^4.$$

A. xanthogrammica. The mean wall thickness of *A. xanthogrammica* body wall near the base of the column (indicated by C in Fig. 6*d*) is $2{\cdot}26 \times 10^{-3}$ m (S.D. = $0{\cdot}56 \times 10^{-3}$ n = 53), hence

$$I_C = \frac{\pi[(3{\cdot}15 \times 10^{-2}\ \text{m})^4 - (2{\cdot}92 \times 10^{-2}\ \text{m})^4]}{4} = 2{\cdot}02 \times 10^{-7}\ \text{m}^4.$$

2. *Shear stress* (σ_s)

Shear stress in a section of an anemone is given by

$$\sigma_s = F/A, \tag{4}$$

where F is the load and A is the cross-sectional area of the beam. The cross-sectional area of a hollow cylinder is given by

$$A = \pi(r_1^2 - r_2^2). \tag{5}$$

M. senile. The force on column section A is assumed to be the drag on the oral disc, and the force on column section B is assumed to be the drag on the entire anemone, hence

$$\sigma_{S_A} = \frac{0{\cdot}37\ \text{N}}{8{\cdot}4 \times 10^{-5}\ \text{m}^2},$$

$$= 4403\ \text{N.m}^{-2}, \text{ and}$$

$$\sigma_{S_B} = \frac{0{\cdot}61\ \text{N}}{4{\cdot}04 \times 10^{-4}\ \text{m}^2},$$

$$= 1510\ \text{N.m}^{-2}.$$

A. xanthogrammica: The force on column section C is assumed to be the drag on the entire anemone, hence

$$\sigma_{S_C} = \frac{0{\cdot}4\ \text{N}}{4{\cdot}39 \times 10^{-4}\ \text{m}^2} = 912\ \text{N.m}^{-2}$$

3. *Maximum tensile stress associated with bending* (σ_T)

The tensile stress (σ_T) in a bending cantilever is given by

$$\sigma_T = \frac{Fxy}{I}, \tag{6}$$

where x is the distance of the section being considered from the free end of the beam (hence Fx is the bending moment of the beam at that section), y is the distance of the area being considered from the centroid of the section (Fig. 1 C), and I is the second moment of area of the section. Maximum tensile stress occurs at the upstream surface in a section of an anemone.

M. senile: the bending moment (Fx) to which section A is subjected is assumed to be due to the drag force acting on the midpoint of the oral disc. The bending moment to which section B is subjected is assumed to be due to the drag acting on the midpoint of the oral disc plus the drag acting on the midpoint of the upper column plus the drag acting on the midpoint of the lower column.

$$\sigma_{T_A} = \frac{(0{\cdot}37\ \text{N})(0{\cdot}12\ \text{m})(2{\cdot}7 \times 10^{-2}\ \text{m})}{3{\cdot}0 \times 10^{-8}\ \text{m}^4} = 39960\ \text{N.m}^{-2},$$

and

$$\sigma_{T_B} = \frac{[(0{\cdot}37\ \text{N})(0{\cdot}33\ \text{m}) + (0{\cdot}10\ \text{N})(0{\cdot}21\ \text{m}) + (0{\cdot}14\ \text{N})(0{\cdot}07\ \text{m})]\ 5{\cdot}9 \times 10^{-2}\ \text{m}}{6{\cdot}9 \times 10^{-7}},$$

$$= 12965\ \text{N.m}^{-2}.$$

A. xanthogrammica. The bending moment to which section C is subjected is assumed to be due to the drag force acting on the midpoint of the oral disc plus the drag force acting on the midpoint of the column, hence

$$\sigma_{T_C} = \frac{[(0{\cdot}24\ \text{N})(0{\cdot}02\ \text{m}) + (0{\cdot}13\ \text{N})(0{\cdot}01\ \text{m})]\ 3{\cdot}15 \times 10^{-2}\ \text{m}}{2{\cdot}02 \times 10^{-7}\ \text{m}^4} = 951\ \text{N.m}^{-2}.$$

4. *Flexural stiffness (EI)*

M. senile. The E of *M. senile* body wall at an extension rate of $0{\cdot}0016\ s^{-1}$ is calculated using equation (1) to be $0{\cdot}17\ MN.m^{-2}$, hence

$$EI_A = (3{\cdot}0 \times 10^{-8}\ m^4)(0{\cdot}17\ MN.m^{-2}) = 0{\cdot}005\ N.m^2$$

and

$$EI_B = (6{\cdot}9 \times 10^{-7}\ m^4)(0{\cdot}17\ MN.m^{-2}) = 0{\cdot}117\ N.m^2.$$

A. xanthogrammica. The E of *A. xanthogrammica* body wall at an extension rate of $0{\cdot}00025\ s^{-1}$ is calcuated using equation (2) to be $0{\cdot}25\ MN.m^{-2}$, hence

$$EI_C = (2{\cdot}02 \times 10^{-7}\ m^4)(0{\cdot}25\ MN.m^{-2}) = 0{\cdot}05\ N.m^2.$$

5. *Deflexion of the oral disc (δ)*

The linear deflexion of the free end of a cantilevered beam is given by

$$\delta = \frac{F(L)^3}{3EI}, \tag{7}$$

where L is the length of the beam.

M. senile. If the deflexion of the oral disc of the *M. senile* is assumed to be due to the drags acting at the midpoints of each of the three portions of the body diagrammed, and if the average of EI_A and EI_B is used as an estimate of EI for the anemone, then by equation (7)

$$\delta = \frac{(0{\cdot}37\ N)(0{\cdot}33\ m)^3 + (0{\cdot}10\ N)(0{\cdot}21\ m)^3 + (0{\cdot}14\ N)(0{\cdot}07\ m)^3}{3(0{\cdot}061\ N.m^{-2})} = 0{\cdot}08\ m.$$

A. xanthogrammica. If deflexion of the oral disc of *A. xanthogrammica* is assumed to be due to the flow forces acting at the midpoints of the oral disc and of the column, and if EI_C is used as an estimate of EI for the anemone, then

$$\delta = \frac{(0{\cdot}24\ N)(0{\cdot}02\ m)^3 + (0{\cdot}13\ N)(0{\cdot}01\ m)^3}{3(0{\cdot}05\ N.m^2)} = 1{\cdot}3 \times 10^{-5}\ m.$$

6. *Critical stress for local buckling (σ_L)*

The stress required to produce local buckling in a hollow cylindrical beam is given approximately by the equation

$$\sigma_L = \frac{0{\cdot}5Et}{D}, \tag{8}$$

where t is the thickness of the beam's wall, D is the diameter of the beam, and $0{\cdot}5$ is an empirically derived coefficient. Thus, although a very wide, thin-walled cylinder has a higher I than a narrower, thicker-walled cylinder of the same cross sectional area, the former would be more likely to undergo local buckling.

M. senile:

$$\sigma_{LA} = \frac{0{\cdot}5(0{\cdot}17\ MN.m^{-2})(5 \times 10^{-4}\ m)}{0{\cdot}054\ m} = 787\ N.m^{-2},$$

and

$$\sigma_{LB} = \frac{0{\cdot}5(0{\cdot}17\ MN.m^{-2})(1{\cdot}1 \times 10^{-3}\ m)}{0{\cdot}118\ m} = 792\ N.m^{-2}.$$

A. xanthogrammica:

$$\sigma_{LB} = \frac{0{\cdot}5(0{\cdot}25\ \mathrm{MN.m^{-2}})(2{\cdot}25 \times 10^{-3}\ \mathrm{m})}{0{\cdot}63\ \mathrm{m}} = 4484\ \mathrm{N.m^{-2}}.$$

Note; The values for σ_S, σ_T, EI and δ reported by Koehl (1976) for specific *M. senile* and *A. xanthogrammica* were calculated as described above: however, the values printed in Table 1 (Koehl, 1976) are in error and should be:

M. senile:

$\sigma_S = 1739\ \mathrm{N.m^{-2}}$, $\sigma_T = 15450\ \mathrm{N.m^{-2}}$, $EI = 0{\cdot}02\ \mathrm{N.m^2}$, $\delta = 6\ \mathrm{cm}$:

A. xanthogrammica:

$\sigma_S = 1075\ \mathrm{N.m^{-2}}$, $\sigma_T = 750\ \mathrm{N.m^{-2}}$, $EI = 1{\cdot}5\ \mathrm{N.m^2}$, $\delta = 0{\cdot}0003\ \mathrm{cm}$.